

# Optimal Design of Reverse Osmosis Module Networks

**Fazilet Maskan, Dianne E. Wiley, and Lloyd P. M. Johnston**

UNESCO Centre for Membrane Science and Technology, School of Chemical Engineering and Industrial Chemistry, The University of New South Wales, Sydney 2052, Australia

**David J. Clements**

School of Electrical Engineering and Telecommunications, The University of New South Wales, Sydney 2052, Australia

*The structure of individual reverse osmosis modules, the configuration of the module network, and the operating conditions were optimized for seawater and brackish water desalination. The system model included simple mathematical equations to predict the performance of the reverse osmosis modules. The optimization problem was formulated as a constrained multivariable nonlinear optimization. The objective function was the annual profit for the system, consisting of the profit obtained from the permeate, capital cost for the process units, and operating costs associated with energy consumption and maintenance. Optimization of several dual-stage reverse osmosis systems were investigated and compared. It was found that optimal network designs are the ones that produce the most permeate. It may be possible to achieve economic improvements by refining current membrane module designs and their operating pressures.*

## Introduction

Reverse osmosis (RO) membrane systems are often used for seawater and brackish water desalination. The systems are typically installed as a network of modules that must be designed to meet the technical, environmental, and economic requirements of the separation process (Edlinger and Gomila, 1996; Henriquez et al., 1991; Noshita, 1994). The complete optimization of an RO network includes the optimal design of both the individual module structure and the network configuration. For a given application, the choice and design of a particular module geometry (that is, plate and frame, tubular, spiral wound, or hollow-fiber modules) depends on a number of factors, including ease and cost of module manufacture, energy efficiency, fouling tendency, required recovery, and capital cost of auxiliary equipment. With suitable transport equations to predict the physical performance of the membrane module, it should be possible to obtain an optimal module structure for any given application. Bhattacharyya et

al. (1992) gave a concise summary of the models for transport across RO membranes for various module types.

While the performance of individual RO modules in terms of operating conditions and module structure has been extensively studied (Sirkar and Rao, 1981; Sirkar et al., 1982; Wiley et al., 1985), the optimal design of RO networks has been less explored. For a fixed industrial module structure, Evangelista (1986), El Halwagi (1992), Voros et al. (1997), and Zhu et al. (1997) have developed design methodologies to optimize RO network configuration and operating conditions.

The present study investigated the complete optimization of an RO network, including the individual module structure, the configuration of the module network, and the operating conditions using constrained nonlinear optimization. Several dual-stage RO network systems were optimized and results pertaining to process economics were compared to identify the optimal network structure. General implications for the optimal design of RO modules and network systems are presented.

Correspondence concerning this article should be addressed to D. E. Wiley.

## Membrane Module Model

The solution diffusion model (Lonsdale et al., 1965) has been shown to be adequate for predicting the local behavior and performance of highly rejecting membranes such as RO membranes (Podall, 1972; Sirkar and Rao, 1981). The flux equations in this two-parameter model are coupled, that is, the solute and solvent transport through membrane depend on the wall concentration, which in turn is a function of solvent and solute fluxes (Sherwood et al., 1965). This results in an implicit flux equation ( $f(J, c_w) = 0$ ), which requires an iterative solution procedure. For highly rejecting membranes with negligible pressure loss in the membrane channel, Rao and Sirkar (1978) simplified the solution diffusion model to an explicit flux equation ( $J = f(c_w)$ ) for tubular modules. Subsequently, using the same assumptions, Sirkar et al. (1982) developed a model for spiral-wound modules and Evangelista (1985) developed a model for hollow-fiber modules in the turbulent flow regime. Evangelista (1986) generalized his equations for membranes with different rejections and developed general design equations applicable for tubular, spiral-wound, and hollow-fiber modules. These models ignore the pressure losses (frictional pressure drop and pressure drop in the module manifolds) inside the modules and are valid for high-pressure systems involving low percentage recovery of permeate per pass, which is common in seawater desalination.

In brackish water applications, where low-pressure operation and high percentage recovery is commonly practiced, frictional pressure loss in the membrane channel cannot be neglected. Wiley et al. (1985) derived flux equations that take into account the frictional pressure drop. They developed a model to determine the optimal module design for tubular, plate and frame, and spiral-wound modules.

The present study used the flux equations from the study of Wiley et al. (1985). However, unlike the previous model, which divided the membrane module into several sections connected in series, the current model treated the module as a single entity and used averaged values of the feed side bulk properties (including concentration, density, viscosity, and diffusivity) to calculate the wall concentration.

Instead of using a linear function to describe the relationship between concentration and osmotic pressure, as is common, the osmotic pressure was calculated from a nonlinear correlation derived from seawater osmotic pressure data (Stoughton and Lieztke, 1965). For concentrations in the range from 0.0004 to 2 molal, the osmotic pressure is given by

$$\pi = 4,540.47c^{0.987}. \quad (1)$$

This nonlinear function is more representative of the entire concentration range encountered during the optimization procedure.

The optimization also took into account the pressure losses in the manifolds of the membrane modules. For tubular modules with tube-side flow, the pressure losses were treated as a series of sudden expansions and contractions from the feed pipe into the module shell and membrane tubes at both the inlet and outlet. The equations describing pressure losses for expansions and contractions, respectively, are (Geankoplis,

1983):

$$DP_{ex} = \left(1 - \frac{A_1}{A_2}\right)^2 \frac{v^2 p}{2\alpha} \quad (2)$$

$$DP_{co} = 0.55 \left(1 - \frac{A_1}{A_2}\right)^2 \frac{v^2 p}{2\alpha}, \quad (3)$$

with  $\alpha = 1$  ( $Re > 2,100$ ) or  $\alpha = 0.5$  ( $Re \leq 2,100$ ).

## Module Configurations

Most module arrangements for RO networks can be categorized as straight-through, tapered, or cascade designs. The straight-through and the tapered arrangements (Evangelista, 1985; Rautenbach and Albrecht, 1989) are multistage module arrangements with several RO modules in parallel in each stage. In the straight-through scheme, the number and size of the modules are identical for every stage, whereas in the tapered flow scheme, the number or the size of the modules decreases over successive stages. Variations of these arrangements include the addition of recycle streams between each stage (Fan et al., 1968, 1969) and the addition of bypass streams (Bansal and Wiley, 1973). These multistage arrangements could involve retentate reprocessing to increase the total permeate flow (Fan et al., 1968, 1969, Bansal and Wiley, 1973) or permeate reprocessing to improve the permeate purity (McCutchan and Goel, 1974; Evangelista, 1989).

Cascade design of RO systems (Kimura et al., 1969; Keurentjes et al., 1992) follows the principles for multistage fractionation columns. In such applications, the process model of a module is divided into two sections; one side of the process model to purify the permeate and the other side to concentrate the retentate. To imitate reflux, there are recycle streams for each stage.

The present study investigated the optimal module design and operating conditions for one- and two-module systems. All possible arrangements of two-module retentate reprocessing schemes, including bypass streams shown in Figures 1–5, were explored. Such retentate reprocessing with bypass schemes is typical of the operation of seawater and brackish water desalination plants. The series arrangement (Figure 1) has been shown to encompass both straight-through and ta-

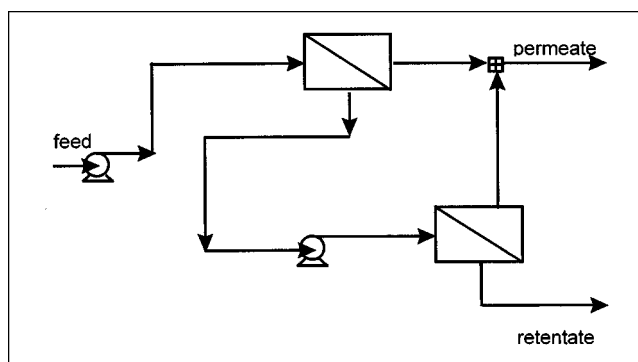


Figure 1. Series configuration.

⊗ : splitter; ⊞ : mixer.

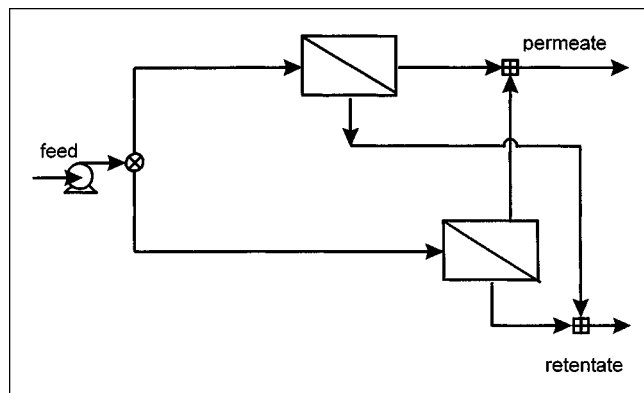


Figure 2. Parallel configuration.

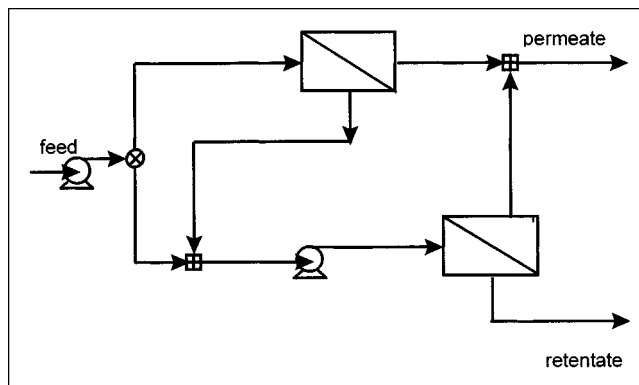


Figure 5. Series with feed bypass.

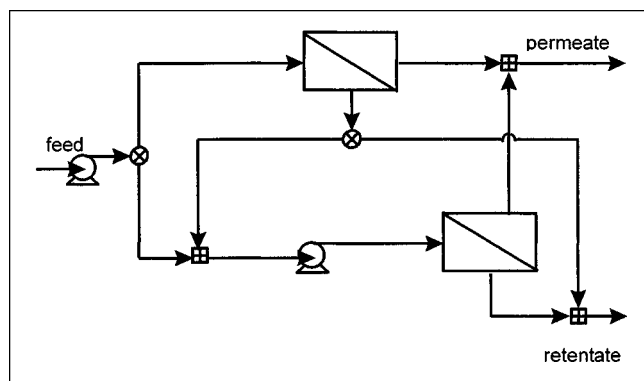


Figure 3. Series with feed and retentate bypass.

pered designs (Evangelista, 1986; El-Halwagi, 1992; Voros, 1997). The single module in each stage can represent several smaller modules in parallel. When the module sizes in both stages are identical, the design is straight through, but when the size decreases, the design is tapered. The mathematical model, which includes pressure losses in piping and fittings, for the RO system was developed using the superset configuration shown in Figure 6, which encompasses all of the other arrangements in Figures 1–5.

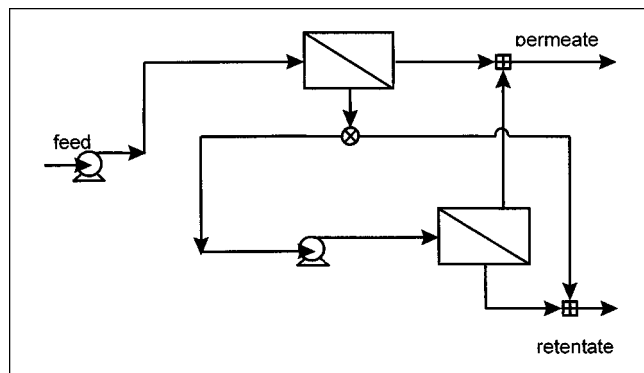


Figure 4. Series with retentate bypass.

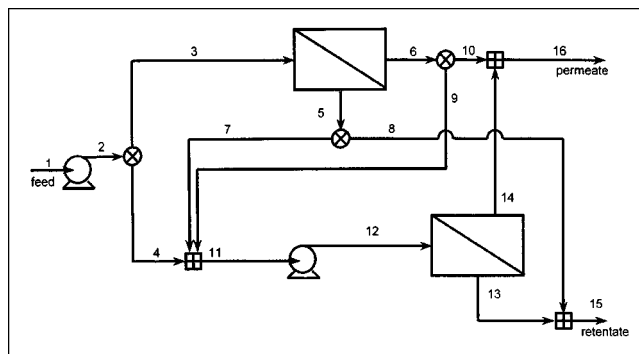


Figure 6. Superset configuration.

### Optimization Procedure

The objective of the design was to maximize  $C_r$ , the yearly profit obtained from the sale of permeate produced by the RO system. The components of the profit calculation are:

1. The income,  $C_{pr}$ , from the “sale” of the permeate based on 350 days/year operation (8,400 h/year):

$$C_{pr} = 8,400 c_{pr} Q_P. \quad (4)$$

The permeate unit profit ( $c_{pr}$ ) should be adjusted to include expenses associated with feed “purchase,” waste disposal, and other operating expenses (such as operational labor costs) not included in other terms in the objective function.

2. The energy (electricity) cost,  $C_e$ , also based on 350 days/year operation:

$$C_e = 8,400 c_e W. \quad (5)$$

3. The annualized capital cost of the membrane module, assuming straight-line depreciation,  $C_m$ , based on a 3-year membrane life and the module area:

$$C_m = 0.33 c_m A. \quad (6)$$

The membrane unit cost ( $c_m$ ) includes the costs of membrane elements, housing, utilities (excluding electricity cost, which

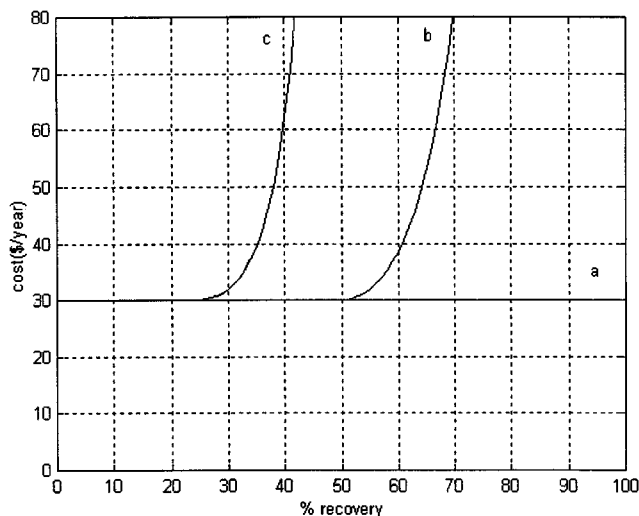


Figure 7. Cleaning and maintenance cost function.

is stated as a separate term), construction, and installation. The effects of different unit lifetimes and costs can be estimated by varying  $c_m$ .

4. The module cleaning and maintenance cost,  $C_r$ , based on the module area:

$$C_r = c_r A. \quad (7)$$

$C_r$  was made a function of the membrane area, since the amount of chemicals and water used for cleaning, pretreatment, and posttreatment; cleaning time; cost of spare parts; labor and membranes are proportional to the size of the RO system. The unit costs ( $c_r$ ) can be fixed or variable. For variable costs,  $c_r$  was defined as a function of permeate recovery per module ( $c_r = f(Q_p/Q_f)$ ). Figure 7 shows the  $c_r$  functions studied. Line a represents a fixed cost, while lines b and c are exponential functions to represent conditions where, due to high permeate recovery, scaling and fouling become serious problems and high chemical usage or more frequent cleaning is required. The lines shown are indicative of costs encountered industrially, but can be adjusted for specific applications.

5. The capital costs of the pump,  $C_p$ , based on the power input and a 10-year pump life, assuming straight-line depreciation:

$$C_p = 0.1 c_{pp} \left( \frac{W}{W_{base}} \right)^m. \quad (8)$$

Then the profit to be maximized is:

$$C_t = C_{pr} - C_e - C_m - C_r - C_p. \quad (9)$$

This objective function allows economic comparison of the module design and arrangements. The effect of changes in cost factors can be investigated by adjusting the unit costs for various terms in the objective function.

The sale of permeate can either be to external or internal customers (including local savings achieved via reduction of

imported site water). In previous studies (Evangelista, 1989; El Halwagi, 1992; and Voros et al., 1997), this term was not included. Sale of either permeate or retentate could be included in the cost function, depending on the purpose of the RO system. Given that the flow rate of the permeate and retentate are complementary, it was only necessary to formally include one of them in the cost function in order to investigate the behavior of the objective function. The inclusion of the profit term also eliminated the need for hard constraints in the optimization.

The objective function depends on a large number of quantities that are separated into variables, with respect to which the function is maximized, and parameters, which are regarded as constants during the optimization calculation. For tubular modules, the variables are the module dimensions (defined by the number of tubes, the tube length, and diameter) and the inlet pressures. For a two-membrane system, there are two sets of module dimensions and inlet pressures. The ranges of the variables studied were:

$$\begin{aligned} P_1 \text{ and } P_2: & 1.2\text{--}15 \text{ MPa}, & d_1 \text{ and } d_2: & 1 \text{ }\mu\text{m}\text{--}2.54 \text{ cm}, \\ l \text{ and } l_2: & 0.1 \text{ mm--}25 \text{ m}, & n_1 \text{ and } n_2: & 1\text{--}1,000,000. \end{aligned}$$

The ranges for module dimensions were chosen to include values typical of tube-side flow tubular or hollow-fiber modules. The range of supply pressures covered typical operating pressures required for brackish and seawater desalination.

All designs required at least one pump for the first membrane module. The inlet pressure to the second membrane module determined whether or not a second pump was required. If the calculated pressure for the feed stream entering the second module was higher than the pressure defined by the optimization procedure, the pump was not used. Otherwise the pump was used to increase the feed pressure.

The optimization parameters are the feed flow, concentration and pressure, membrane permeability and salt rejection, unit costs for the membrane, electricity, and membrane cleaning and maintenance, and the permeate sale price. The values of parameters studied were:

$$\begin{aligned} Q_f: & 1.39 \times 10^{-3} \text{ m}^3/\text{s}, & c_m: & 10\text{--}200 \text{ } \$/\text{m}^2, \\ c_f: & 4,000 \text{ and } 35,000 \text{ ppm TDS}, & c_e: & 5\text{--}10 \text{ c/kWh}, \\ P_f: & 98.1 \text{ kPa}, & c_{pr}: & 0.5\text{--}1 \text{ } \$/\text{m}^3, \\ A_m: & 2.21 \times 10^{-9} \text{ m}/(\text{s} \cdot \text{kPa}), & c_r: & 30 \text{ } \$/\text{m}^2 \cdot \text{year} \text{ (fixed cost;} \\ R: & 99.5 \%, & & \text{for variable cost see Figure 7).} \end{aligned}$$

The system model was coded in MATLAB and optimized using the sequential quadratic programming method. The optimization was performed on an IBM pentium PC (200 MHz) using MATLAB, and typically took 10–410 s CPU time per run, depending on the initial values used for the optimized variables.

## Results and Discussion

### Generalized findings

For both seawater, and brackish water feeds, Table 1 shows that the optimal module design is many short, thin tubes.

**Table 1. Optimization Result for Seawater and Brackish Water Feed**

Arrangement	Feed: Seawater; $c_p$ : a						Feed: Brackish Water; $c_p$ : a					
	Fig. 1	Fig. 5	Fig. 3	Fig. 4	Fig. 2	Single Module	Fig. 1	Fig. 5	Fig. 3	Fig. 4	Fig. 2	Single Module
<i>Module 1</i>												
$P_f$ MPa	14.2	14.1	14.1	13.9	14.0	14.0	7.94	8.15	8.30	8.20	8.31	8.31
$l$ m	0.064	0.018	0.044	0.42	0.070	0.11	0.057	0.027	0.045	0.086	0.064	0.10
$d$ cm	0.061	0.036	0.030	0.10	0.024	0.030	0.046	0.044	0.036	0.038	0.028	0.036
$n$	$3.0 \times 10^5$	$10^6$	$10^6$	$10^6$	$10^6$	$10^6$	$10^6$	$10^6$	$10^6$	$10^6$	$10^6$	$10^6$
Membr. area (m <sup>2</sup> )	37.8	20.6	41.9	99.3	52.2	104	82.1	36.9	50.6	104	56.3	113
Recovery (%)	54.8	57.8	79.0	80.9	81.6	81.6	82.9	78.7	92.1	92.1	93.7	93.7
<i>Module 2</i>												
$P_f$ MPa	14.2	14.1	14.1		14.0		7.94	8.15	8.30	8.20	8.31	
$l$ m	0.070	0.092	0.078		0.070		0.041	0.079	0.069	0.015	0.064	
$d$ cm	0.025	0.028	0.025		0.024		0.021	0.030	0.028	0.013	0.028	
$n$	$10^6$	$10^6$	$10^6$		$10^6$		$10^6$	$10^6$	$10^6$	$10^6$	$10^6$	
Membr. area (m <sup>2</sup> )	54.8	79.8	61.2		52.2		26.4	74.5	58.4	6.28	56.3	
Recovery (%)	61.9	75.3	76.2		81.6		75.6	91.0	92.0	51.7	93.7	
Total profit (\$/y)	$1.68 \times 10^4$	$1.64 \times 10^4$	$1.58 \times 10^4$	$1.59 \times 10^4$	$1.59 \times 10^4$	$1.59 \times 10^4$	$2.73 \times 10^4$	$2.64 \times 10^4$	$2.59 \times 10^4$	$2.63 \times 10^4$	$2.59 \times 10^4$	$2.59 \times 10^4$
Total recovery (%)	82.8	82.4	81.6	80.9	81.6	81.6	95.8	94.6	93.9	94.5	93.7	93.7

Note:  $c_p$ : 0.05 \$/kWh;  $c_{pr}$ : 1 \$/m<sup>3</sup>;  $c_m$ : 50 \$/m<sup>2</sup>.

Usually, the optimum number of tubes is the maximum allowable value. A large number of tubes means that the cross-flow velocity in each tube is as small as possible, which helps reduce the frictional pressure drop. This agrees with results reported by Wiley et al. (1985), that the optimum design of a single module is achieved by keeping the crossflow low. The frictional pressure drop is further lowered with short tube length and large diameter. However, large diameter reduces the solute mass-transfer coefficient, which in turn increases the solute wall concentration and the osmotic pressure. The balance between these effects produces a module with short, thin tubes, which was also reported in the previous study (Wiley et al., 1985). While not typical of industrial practice, the number and diameter of tubes is suggestive of a tube-side flow hollow-fiber system, although the optimum length is generally shorter.

On average, Table 1 shows that the permeate recovery for brackish water feed is higher than for seawater feed. This is not unexpected, since solutions of lower salt concentration have lower osmotic pressure. Therefore for the same supply pressure, the brackish water system has a higher effective transmembrane pressure than the seawater system.

The inclusion of permeate profit in the objective function drives the optimal design in a direction that produces a large volume of permeate to offset capital and operational costs. High permeate volume can be achieved by applying high transmembrane pressure and/or increasing the membrane area. Energy and membrane costs balance increases in supply pressure and membrane area. The optimum operating points for both feeds is at very high supply pressure, leading to high permeate production. For all cases considered, including ones not shown in the tables, the optimum supply pressure for seawater feed is in the range 9–15 MPa, while for brackish water feed the range is 4.5–8.5 MPa. The optimum membrane area for both feed concentrations is within the range for typical commercial hollow-fiber or spiral-wound modules (20–150 m<sup>2</sup>/module).

Such high permeate recovery produced using high supply pressure was also reported in the optimization study by Voros

et al. (1997), who used a different system model and objective function to optimize the design of RO desalination plants. However, they arrived at an optimum design that maximized the permeate production by maximizing the supply pressure and minimizing the membrane area. In their study, the supply pressure was limited to typical membrane manufacturer's specifications that arise from the maximum pressure the membrane can withstand and the cost of pressure vessels. The optimum operating pressure obtained was at the upper pressure limit. In the work presented here the upper limit for the supply pressure was increased and it is found that mathematically, the optimum operating pressure is higher than that used in current practice, typically in the range 1.4–4.2 MPa for brackish water, and 5–8.5 MPa for seawater desalination.

### Effect of unit costs

All results in Table 1 show that optimum designs produce a large volume of permeate. Although it is economically desirable, current RO systems normally operate at lower permeate recovery, since high recovery requires more intensive membrane cleaning and maintenance procedures and more extensive feed pretreatment, which means increased capital and operating costs. To study these effects, the cleaning and maintenance unit cost was made a function of the membrane module's permeate recovery. The shape of the cleaning and maintenance cost functions ( $c_r$ ) shown in Figure 7 effectively change permeate recovery. For example, from Table 2, when  $c_r$  takes the form of line a, the recovery per module is 55–82% for seawater feed and 52–94% for brackish water. However, if  $c_r$  takes the form of line b, the recovery is 60–66% for brackish water, and if  $c_r$  has the form of line c for seawater, the recovery is 37–38%. These changes in recoveries, however, do not change the trend of the optimum module design, that is, short, thin tubes resembling a tube-side feed hollow-fiber system.

Higher permeate unit profit and/or lower electricity unit cost result in a design where more feed is recovered as permeate. When the optimum permeate recovery decreases due

**Table 2. Effect of Cleaning and Maintenance Cost Function on % Recovery**

Arrangement Module	Fig. 1		Fig. 5		Fig. 3		Fig. 4		Fig 2
	1	2	1	2	1	2	1	2	1&2
<i>Seawater, <math>c_r</math> function: a</i>									
$Q_f$ (m <sup>3</sup> /s)	$1.4 \times 10^{-3}$	$6.4 \times 10^{-4}$	$6.9 \times 10^{-4}$	$1.0 \times 10^{-3}$	$6.9 \times 10^{-4}$	$7.8 \times 10^{-3}$	$1.4 \times 10^{-3}$	$1.8 \times 10^{-4}$	$6.9 \times 10^{-4}$
$c_f$ (mol/kg)	0.60	1.3	0.60	0.84	0.60	0.81	0.60	2.23	0.60
Module recovery	55 %	62 %	58 %	75 %	79 %	76 %	81 %	0 %	82 %
Total recovery	83%		82%		82%		81%		82%
Profit (\$/yr)	$1.68 \times 10^4$		$1.64 \times 10^4$		$1.58 \times 10^4$		$1.59 \times 10^4$		$1.59 \times 10^4$
<i>Seawater, <math>c_r</math> function: c</i>									
$Q_f$ (m <sup>3</sup> /s)	$1.4 \times 10^{-3}$	$8.6 \times 10^{-4}$	$6.9 \times 10^{-4}$	$1.1 \times 10^{-3}$	$6.9 \times 10^{-4}$	$9.2 \times 10^{-4}$	$1.4 \times 10^{-3}$	$4.4 \times 10^{-4}$	$6.9 \times 10^{-4}$
$c_f$ (mol/kg)	0.60	0.96	0.60	0.73	0.60	0.68	0.60	0.97	0.60
Module recovery	38 %	38 %	37 %	38 %	38 %	38 %	38 %	36 %	38 %
Total recovery	61 %		50 %		44 %		49 %		38 %
Profit (\$/yr)	$1.09 \times 10^4$		$7.43 \times 10^3$		$5.71 \times 10^3$		$7.28 \times 10^3$		$4.11 \times 10^3$
<i>Brackish water, <math>c_r</math> function: a</i>									
$Q_f$ (m <sup>3</sup> /s)	$1.4 \times 10^{-3}$	$2.5 \times 10^{-4}$	$6.9 \times 10^{-4}$	$8.3 \times 10^{-4}$	$6.9 \times 10^{-4}$	$7.2 \times 10^{-4}$	$1.4 \times 10^{-3}$	$5.6 \times 10^{-5}$	$6.9 \times 10^{-4}$
$c_f$ (mol/kg)	0.068	0.40	0.068	0.11	0.068	0.10	0.068	0.86	0.068
Module recovery	83 %	76 %	79 %	91 %	92 %	92 %	92 %	52 %	94 %
Total recovery	96 %		95 %		94 %		94 %		94 %
Profit (\$/yr)	$2.73 \times 10^4$		$2.64 \times 10^4$		$2.59 \times 10^4$		$2.63 \times 10^4$		$2.59 \times 10^4$
<i>Brackish water, <math>c_r</math> function: b</i>									
$Q_f$ (m <sup>3</sup> /s)	$1.4 \times 10^{-3}$	$5.6 \times 10^{-4}$	$6.9 \times 10^{-4}$	$9.7 \times 10^{-4}$	$6.9 \times 10^{-4}$	$8.3 \times 10^{-4}$	$1.4 \times 10^{-3}$	$2.5 \times 10^{-4}$	$6.9 \times 10^{-4}$
$c_f$ (mol/kg)	0.068	0.17	0.068	0.10	0.068	0.09	0.068	0.19	0.068
Module recovery	60 %	65 %	60 %	66 %	63 %	65 %	64 %	64 %	66 %
Total recovery	86 %		76 %		70 %		75 %		66 %
Profit (\$/yr)	$2.34 \times 10^4$		$1.95 \times 10^4$		$1.74 \times 10^4$		$1.93 \times 10^4$		$1.55 \times 10^4$

Note:  $c_e$ : 0.05 \$/kWh;  $c_{pr}$ : 1 \$/m<sup>3</sup>;  $c_m$ : 50 \$/m<sup>2</sup>.

to increased capital or operating costs, either supply pressure or membrane area decreases (Table 3). Most often the supply pressure is maintained at a relatively high value, while the membrane area is decreased. This shows that maintaining a high supply pressure is less costly than, and preferable to, increasing membrane area in maintaining high permeate production.

Table 3 also shows that the total profit is very sensitive to permeate unit price, with a 25% decrease in permeate price resulting in a 53% decrease in profit. Between capital and operating costs, the total profit is more sensitive to changes in electricity unit cost (operating cost) than membrane unit price (capital cost). When the electricity unit price is doubled (0.05 to 0.1 \$/kWh), the total profit decreases 65%, while a ten times increase in membrane unit price (10 to 100 \$/m<sup>2</sup>) results in only a 22% decrease in profit. From the cost breakdown in Figure 8, it is clear that electricity is the biggest cost component, followed by membrane costs and pump costs. The data in Figure 8 are typical of results at all conditions. Electricity cost dominates because of the high pressure of the optimal designs.

For the optimization of the RO system profit, the objective function has two optima. One optimum is the design that produces a lot of permeate, and the other optimum is the design that produces no permeate. Normally, the design that produces permeate is the global optimum. With increasing unit costs and decreasing permeate price, the total profit of the system declines. Figure 9 shows that the effect of increasing membrane unit price is to reduce the total profit until a point is reached where the sale of permeate is not enough to offset the capital and operating costs. At this point the global optimum is the design that does not produce any permeate, and such a separation process would be carried out at an overall cost to a business. If the feed solution was an effluent, it would be cheaper to pay the waste disposal cost under these conditions than to build and operate a membrane plant to treat the waste.

### Effect of module configuration

For both feed concentrations and all unit costs, the series arrangement (Figure 1) has the largest permeate profit. The

**Table 3. Sensitivity Analysis for Electricity, Membrane, and Permeate Unit Prices**

Electricity price (\$/kWh)	0.1	0.05	0.05	0.05	0.05	0.5
Permeate price (\$/m <sup>3</sup> )	1.0	0.50	0.75	1.0	1.0	1.0
Memb. price (\$/m <sup>2</sup> )	50	50	50	50	10	100
$P_f$ (MPa)	9.92	10.9	12.7	14.0	13.2	14.7
$P_{effective}$ (MPa)	3.54	4.91	5.15	5.27	4.47	6.13
Total memb. area (m <sup>2</sup> )	139	97.6	102	104	124	89.6
Total recovery (%)	73.0	71.0	78.1	81.6	81.8	81.4
Profit (\$/y)	$5.52 \times 10^3$	−345	$7.53 \times 10^3$	$1.59 \times 10^4$	$1.74 \times 10^4$	$1.43 \times 10^4$

Note: Feed: seawater, arrangement: parallel (Figure 2);  $c_r$  cost function: a

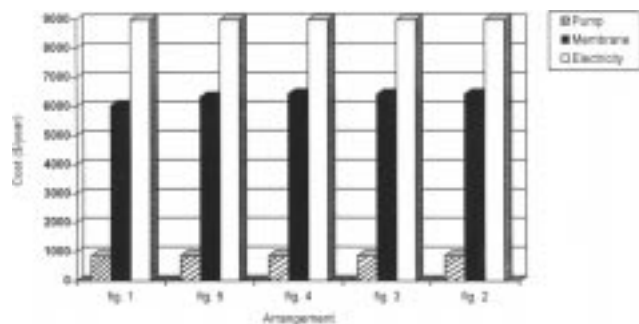


Figure 8. Cost breakdown.

Feed: seawater,  $c_e$ : 0.05 \$/kWh;  $c_{pr}$ : 1 \$/m<sup>3</sup>,  $c_m$ : 50 \$/m<sup>2</sup>,  $c_r$  cost function:  $a$ .

series with the feed bypass arrangement (Figure 5) has the second largest profit. Table 4 shows that the optimum design for two parallel modules and a single module are essentially the same for both feeds. The total membrane area and module inlet pressure are identical. The difference in the total profit arises because the parallel arrangement has more piping and fittings in the system, causing more pressure loss, than in a single module. Theoretically, it is therefore more profitable to have one big module instead of several smaller ones in parallel. In practice, however, parallel arrangements cannot be avoided, since there is a technical and engineering limit to the construction of large membrane modules.

In optimum two stage arrangements, the use of a second pump is usually avoided. The design is such that the pressure losses in the first module and the fittings are negligible compared to the supply pressure. In some brackish water cases, the second pump is introduced when the second module operating pressure is higher than 9 MPa. In this case, the capital cost of the second pump is offset by the additional amount of permeate produced from the second module at enhanced pressure.

The difference in the total permeate recovery between all arrangements for fixed feed concentration and unit prices is small (such as Table 1). When the permeate recovery per module is limited by the cleaning and maintenance cost (that is, taking the form of lines b and c in Figure 7), the variation in total recovery between arrangements is wider (such as Table 2).

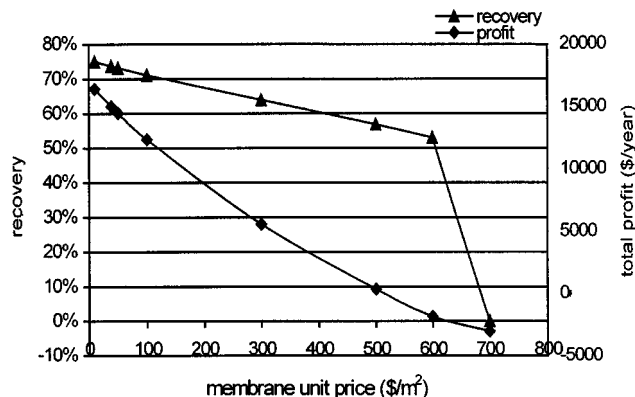


Figure 9. Permeate recovery as a function of membrane unit price.

Feed: seawater, arrangement: Parallel (Figure 2).  $c_e$ : 0.05 \$/kWh;  $c_{pr}$ : 1 \$/m<sup>3</sup>,  $c_r$  cost function:  $a$ .

For constant cleaning and maintenance costs and seawater feed, the optimum two-stage arrangement with retentate bypass only (Figure 4) has the same profit as the optimum single-module arrangement. In the series arrangement, permeate recovery is balanced between the first and second modules. The addition of a retentate bypass stream increases premeate recovery in the first module, and the second module becomes so small that the design of the two-stage retentate bypass arrangement emulates the design of a single module. The two-stage arrangement with both feed and retentate bypass streams (Figure 3) is the least profitable and has a smaller total permeate recovery than the single-stage arrangement. In this two-stage arrangement, even though the recovery in the first module increases above that for the series arrangement, the second module is still required because the retentate is diluted with the feed bypass stream.

For brackish water feed, both two-stage arrangements with retentate bypass streams (Figures 3 and 4) produce greater profit than single-stage arrangements. The retentate concentration for the first module in both these two-stage arrangements is relatively low and the second module can still produce permeate, although for the arrangement with retentate bypass only (Figure 4) the permeate flow is small.

For both feeds when the permeate recovery per module is limited by variable cleaning and maintenance costs, the re-

Table 4. Comparison between a Single Module and Two Parallel Modules Designs

Feed		Seawater		Brackish Water	
Arrangement		Two Parallel Modules	One Module	Two Parallel Modules	One Module
$P$	MPa	14.0	14.0	8.31	8.31
$P_{\text{effective}}$	MPa	5.27	5.27	5.62	5.62
$P_{\text{brine}}$	MPa	14.0	14.0	8.31	8.31
$l$	m	0.0704	0.110	0.064	0.100
$d$	cm	0.0236	0.0301	0.028	0.036
$n$		$10^6$	$10^6$	$10^6$	$10^6$
Total memb. area (m <sup>2</sup> )		104	104	113	113
$c_w$	(mol/kg)	1.92	1.92	0.58	0.58
Total recovery		81.6%	81.6%	93.7%	93.7%
Total profit (\$/yr)		$1.59 \times 10^4$	$1.59 \times 10^4$	$2.59 \times 10^4$	$2.59 \times 10^4$

$c_e$ : 0.05 \$/kWh;  $c_{pr}$ : 1 \$/m<sup>3</sup>;  $c_m$ : 50 \$/m<sup>2</sup>.

covery in the first module in all arrangements is almost the same, and consequently the retentate concentration leaving the first module is almost identical. In this case, feed concentration does not affect the optimum design, but the total volume of feed processed by the two modules (that is,  $Q_3 + Q_{12}$  in Figure 6) does. Generally, the optimum design is greatly affected by the amount of permeate produced. The most profitable system is the one that produces the most permeate. If the total value of  $(Q_3 + Q_{12})$  is high, more permeate is produced and the permeate profit is greater. Two-stage arrangements, with or without bypass streams, always had higher  $(Q_3 + Q_{12})$  than a single-stage arrangement. Bypass streams in two-stage processing lessens permeate production and reduces profitability. However, high permeate production in two-stage systems results in higher permeate solute concentration than it does in single-stage systems. If the final permeate concentration is above a required concentration, bypass streams are useful in keeping the permeate concentration below the limit while maintaining high permeate production.

### Nature of the objective function

Some case studies show that when the optimization is carried out using different initial guesses, the objective function converges to several local maxima. In the optimization of the series and series with retentate bypass arrangements (Figures 1 and 4), a single module design is observed as a local maximum. In the optimization of the series arrangement, the single module design never becomes the global maximum, but in the optimization of series with a retentate bypass arrangement, the single module and two-module designs compete to be the global maximum. With seawater feed, the single-module design is the global maximum, while with brackish water feed the two-module design is the global maximum.

The single-module design maximum is not observed in the optimization of series arrangements with feed bypass stream (Figures 3 and 5). This is because it is impossible to obtain an optimum design that emulates other arrangements with fixed

split ratios in splitters H and I (Figure 6). When the split ratios are optimized along with the other parameters, the optimum design is the series arrangement (Figure 1). This confirms that the series arrangement is the most profitable arrangement.

The plot of the objective function ( $C_f$ ) against the module's length ( $l$ ) and number of tubes ( $n$ ) (Figure 10) shows that the function is relatively flat along the  $n$ -axis. Other plots of the function  $C_f$  against diameter and number of tubes (not shown here) are also flat along the  $n$ -axis, and the plot against length and diameter is flatter along the length axis. The optimum module design is therefore, relatively insensitive to changes in number of tubes and more sensitive to changes in tube length or diameter. This is because with short and small tubes, the pressure drop in the membrane module is minimal, and a relatively small change in the number of tubes or tube length is negligible in a high-pressure system. This is reflected in the optimization results for parallel and single-module designs (Table 4) where both designs have different module dimensions but similar membrane area, transmembrane pressure, and wall concentration.

### Conclusion

The optimum module design for desalination applications has many small, short channels and operates at high permeate recovery with high operating pressure and low cross-flow velocity. For the same membrane area, it is preferable to have a lot of short channels in parallel rather than long channels in series. Such a design minimizes concentration polarization and frictional pressure drop inside each module.

The optimization of RO networks is affected by feed concentration and permeate recovery per module. Optimal networks are more profitable because they produce more permeate than nonoptimal networks. Staged retentate reprocessing produces more permeate than single-stage arrangements, while bypass streams reduce permeate recovery. Of the networks considered, the series arrangement is the most economical.

Increasing operating pressure achieves greater profitability than increasing membrane area. Thus, reduction in operating costs is more important than reduction in capital costs in increasing profitability, and electricity costs are the dominant cost factor.

While design and operation of membrane systems have improved significantly since the development of the first applications, optimization theory can still offer insights that can further improve the systems. Current commercial module designs that approach the optimum module dimensions are spiral wound and tube-side feed hollow-fiber modules, although the length of the channel in these modules, could be further refined subject to technical and manufacturing constraints. Similarly, significant economic improvements might be achievable for RO processes if it is possible to reengineer RO modules and networks to operate at higher pressures than in current practice.

### Notation

$A$  = membrane area,  $m^2$   
 $A_m$  = membrane permeability,  $m/(s \cdot kPa)$   
 $A_1$  = smaller pipe cross-sectional area,  $m^2$

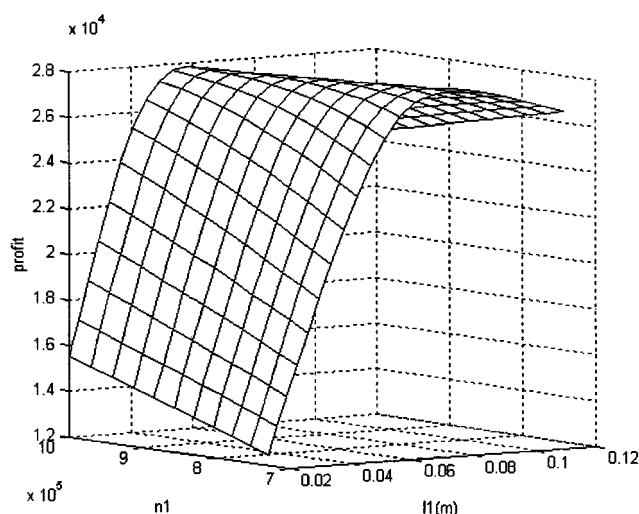


Figure 10. Objective function plotted against  $n_1$  and  $l_1$ .

Series arrangements, feed: brackish water,  $c_s$ : 0.05 \$/kWh;  $c_m$ : 35 \$/m<sup>2</sup>;  $c_{pr}$ : 1 \$/m<sup>3</sup>;  $c_r$  cost function:  $a$ .



$A_2$  = larger pipe cross-sectional area,  $m^2$   
 $c_f$  = feed concentration, mol/kg  
 $c_w$  = wall concentration, mol/kg  
 $c_{pp}$  = pump cost, \$  
 $d$  = diameter, m  
 $J$  = flux, m/s  
 $m$  = exponent in pump cost equation  
 $P$  = pressure, kPa  
 $Q$  = flow rate,  $m^3/s$   
 $R$  = membrane rejection  
 $v$  = velocity, m/s  
 $W$  = work, kW  
 $\rho$  = density,  $kg/m^3$

## Literature Cited

- Bansal, I. K., and A. J. Wiley, "A Mathematical Model for Optimizing the Design of Reverse Osmosis Systems," *TAPPI*, **56**, 112 (1973).
- Bhattacharyya, D., M. E. Williams, R. J. Ray, and S. B. McCray, "Reverse Osmosis: Design," *Membrane Handbook*, W. S. W. Ho and K. K. Sircar, eds., Van Nostrand Reinhold, New York (1992).
- Edlinger, R. and F. Z. Gomila, "Ibiza Seawater RO—Special Design Features and Operating Data," *Desalination*, **105**, 125 (1996).
- El-Halwagi, M. M., "Synthesis of Reverse-Osmosis Networks for Waste Reduction," *AIChE J.*, **38**, 1185 (1992).
- Evangelista, F., "A Short Cut Method for the Design of Reverse Osmosis Desalination Plants," *Ind. Eng. Chem. Process Des. Dev.*, **24**, 211 (1985).
- Evangelista, F., "Improved Graphical Analytical Method for the Design of Reverse Osmosis Desalination Plants," *Ind. Eng. Chem. Process Des. Dev.*, **25**, 366 (1986).
- Fan, L. T., C. L. Hwang, L. E. Erickson, C. Y. Cheng, and L. Y. S. Ho, "Analysis and Optimization of a Reverse-Osmosis Water Purification Systems: I. Process Analysis and Simulation," *Desalination*, **5**, 237 (1968).
- Fan, L. T., C. L. Hwang, L. E. Erickson, C. Y. Cheng, and L. Y. S. Ho, "Analysis and Optimization of a Reverse-Osmosis Water Purification System: II: Optimization," *Desalination*, **6**, 131 (1969).
- Geankoplis, Christie J., *Transport Processes and Unit Operations*, Allyn and Bacon, Boston (1983).
- Henriquez, J. F., J. Bonet, and J. Etzaniz, "Galdar-Agaete Seawater Desalination Plant Construction and One Year Operational Experience for the 3,500  $m^3/day$  RO Plant," *Desalination*, **82**, 71 (1991).
- Keurentjes, J. T. F., L. J. M. Linders, W. A. Beverloo, and K. Van't Riet, "Membrane Cascades for the Separation of Binary Mixtures," *Chem. Eng. Sci.*, **47**, 1561 (1992).
- Kimura, S., S. Sourirajan, and H. Ohya, "Stagewise Reverse-Osmosis Process Design," *Ind. Eng. Chem. Process Des. Dev.*, **8**, 79 (1969).
- Lonsdale, H. K., U. Merten, and R. L. Riley, "Transport Properties of Cellulose Acetate Membranes," *J. Appl. Polym. Sci.*, **9**, 1341 (1965).
- McCutchan, J. W., and V. Goel, "System Analysis of a Multistage Tubular Module Reverse-Osmosis Plant for Sea-Water Desalination," *Desalination*, **14**, 57 (1974).
- Noshita, M., "Reverse Osmosis Seawater Desalination for Power Plant," *Desalination*, **96**, 359 (1994).
- Podall, H. E., "Reverse Osmosis," *Recent Development in Separation Science*, N. N. Li, ed., Vol. II, CRC Press, Cleveland, OH (1972).
- Rao, G. H., and K. K. Sircar, "Explicit Flux Expressions in Tubular Reverse Osmosis Desalination," *Desalination*, **27**, 99 (1978).
- Rautenbach, R., and R. Albrecht, *Membrane Processes*, Wiley, New York (1989).
- Sherwood, T. K., P. L. T. Brian, R. E. Fisher and L. Dresner, "Salt Concentration at Phase Boundaries in Desalination by Reverse Osmosis," *Ind. Eng. Chem. Fundam.*, **4**, 113 (1965).
- Sircar, K., P. T. Dang, and G. H. Rao, "Approximate Design Equations for Reverse Osmosis Desalination by Spiral Wound Modules," *Ind. Eng. Chem. Process Des. Dev.*, **27**, 517 (1982).
- Sircar, K., and G. H. Rao, "Approximate Design Equations and Alternate Design Methodologies for Tubular Reverse Osmosis Desalination," *Ind. Eng. Chem. Process Des. Dev.*, **20**, 116 (1981).
- Stoughton, R. W., and M. H. Lietzke, "Calculation of Some Thermodynamic Properties of Sea Salt Solutions at Elevated Temperatures from Data on NaCl Solutions," *J. Chem. Eng. Data*, **10**, 254 (1965).
- Voros, N. G., Z. B. Maroulis, and D. Marinos-Kouris, "Short-Cut Structural Design of Reverse Osmosis Desalination Plants," *J. Memb. Sci.*, **127**, 47 (1997).
- Wiley, D. E., A. G. Fane, and C. J. D. Fell, "Optimisation of Membrane Design for Brackish Water Desalination," *Desalination*, **52**, 249 (1985).
- Zhu, M., M. M. El-Halwagi, and M. Al-Ahmad, "Optimal Design and Scheduling of Flexible Reverse Osmosis Networks," *J. Memb. Sci.*, **129**, 161 (1997).

Manuscript received May 24, 1999, and revision received Jan. 3, 2000.